

Photometric study of distant open clusters in the second quadrant: NGC 7245, King 9, King 13 and IC 166

Annapurni Subramaniam¹★ and Bhuwan Chandra Bhatt²★

¹Indian Institute of Astrophysics, Bangalore 560034, India

²CREST Campus, Indian Institute of Astrophysics, PO Box 19, Hosakote, Bangalore 562114, India

Accepted 2007 February 20. Received 2007 February 19; in original form 2006 September 20

ABSTRACT

We present a *UBV* CCD photometric study of four open clusters, NGC 7245, King 9, IC 166 and King 13, located between $l = 90^\circ$ and 135° . All are embedded in a rich Galactic field. NGC 7245 and King 9 are close together in the sky and have similar reddenings. The distances and ages are: NGC 7245, 3.8 ± 0.35 kpc and 400 Myr; King 9 (the most distant cluster in this quadrant), 7.9 ± 1.1 kpc and 3.0 Gyr. King 13 is 3.1 ± 0.3 kpc distant and 300 Myr old. King 9 and IC 166 (4.8 ± 0.5 kpc distant and 1 Gyr old) may be metal-poor clusters ($Z = 0.008$), as estimated from isochrone fitting. The average value of the distance of young clusters from the Galactic plane in the above longitude range and beyond 2 kpc (-47 ± 16 pc, for 64 clusters) indicates that the young disc bends towards the southern latitudes.

Key words: open clusters and associations: individual: NGC 7245 – open clusters and associations: individual: King 9 – open clusters and associations: individual: King 13 – open clusters and associations: individual: IC 166.

1 INTRODUCTION

Open star clusters are the best testing ground for stellar evolution, Galactic structure and chemical evolution of the disc. To increase the sample of clusters beyond the 2 kpc radius in the second quadrant, we observed four clusters, NGC 7245, King 9, King 13 and IC 166 with poorly known parameters.

2 PREVIOUS STUDIES

Yilmaz (1970) presented RGU photographic photometry of NGC 7245 [right ascension (RA) (2000) 22:15:11, Declination (Dec.) (2000) +54:20:36; $l = 101^\circ 368$, $b = -1^\circ 852$] and obtained a distance of 1925 pc and a reddening of 0.60 mag. WEBDA presents the *UBV* photographic photometry by Karaali (1971) and CCD photometry by Petry & DeGioia-Eastwood (private communication) for 67 stars. According to WEBDA, the cluster is at a distance of 2106 pc, reddening is of 0.473 mag and $\log(\text{age})$ is 8.246. Viskum et al. (1997) performed *BV* CCD photometry of 650 stars in a 7.7×7.7 -arcmin² region around NGC 7245 to detect δ Scuti stars. Using isochrone fitting, they estimated the age as 320 Myr, reddening of $E(B - V) = 0.40 \pm 0.02$ and distance as 2800 pc.

None of the parameters is estimated for King 9 in the literature (RA 22:15:30, Dec. +54:24:00). *VI* CCD photometry was performed by Phelps, Janes & Montgomery (1994), but no parameters

were estimated. This is the first calibrated photometric study of King 9 in *U* and *B* bands and the first estimation of cluster parameters.

Marx & Lehmann (1979) obtained *UBV* photographic photometry of King 13 (RA 00:10:06, Dec. +61:10:00) and estimated the distance as 1730 pc. IC 166 (RA 01:52:30, Dec. +61:50:00) is a faint and distant cluster. Burkhead (1969) obtained photographic photometry of about 200 stars and photoelectric photometry of 20 stars in the central region. Assuming a reddening of $E(B - V) = 0.8$ mag, the distance was estimated as 3.3 kpc. WEBDA presents the distance as 3970 pc, reddening as 1.05 mag and $\log(\text{age})$ as 8.63. From *JHK*-infrared photometry, Vallenari, Carraro & Richichi (2000) estimated the age as ~ 1 Gyr, reddening $(B - V) = 0.50$ mag and distance $\cong 4.5$ kpc.

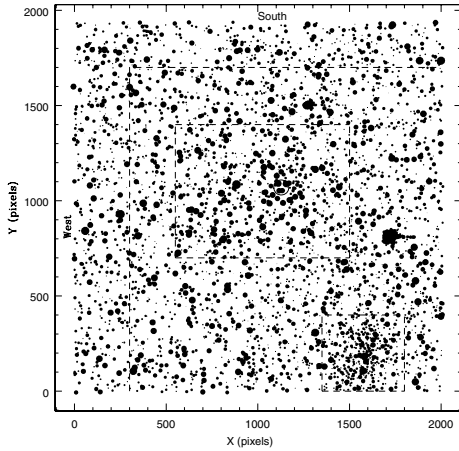
3 OBSERVATIONS

Data were obtained using the 2-m Himalayan Chandra Telescope (HCT), Hanle, IAO, operated by the Indian Institute of Astrophysics. The instrument used is the imaging camera of the Himalayan Faint Object Spectrograph and Camera (HFOSC). The details of the telescope and the instrument are available from the web site, http://www.iiap.res.in/centres_iao.htm. The CCD used for imaging is a $2\text{ k} \times 4\text{ k}$ CCD, where the central $2\text{ k} \times 2\text{ k}$ pixels were used for imaging. The pixel size is $15\ \mu\text{m}$ with an image scale of $0.297\ \text{arcsec pixel}^{-1}$. The total area observed is approximately 10×10 arcmin². The log of observations is given in Table 1. NGC 7245 and King 9 are imaged in the same frame and hence they have the same log of observations. The nights of observations were photometric and Landolt standards were observed for photometric

★E-mail: purni@iiap.res.in (AS); bcb@crest.ernet.in (BCB)

Table 1. Log of photometric observations.

Cluster	Date	Filter	Exposure time (s)
NGC 7245/King 9	2003 September 19	<i>V</i>	1, 10, 60, 120
		<i>B</i>	10, 30, 300
		<i>U</i>	60, 2 × 300
IC 166	2003 September 19	<i>V</i>	10, 60, 120
		<i>B</i>	30, 180, 300
		<i>U</i>	180, 600
King 13	2003 September 18	<i>V</i>	5, 30, 60
		<i>B</i>	10, 60, 300
		<i>U</i>	180, 600

**Figure 1.** The observed region of the cluster NGC 7245. The cluster area of NGC 7245, King 9 (lower right-hand side) and field regions considered as control fields are indicated by the dashed lines.

calibrations. The seeing was between 1 and 1.5 arcsec. The initial CCD reductions were carried out using IRAF. DAOPHOT II (Stetson 1987) was used for magnitude estimation and calibration. The transformation equations used are

$$u = U + 3.447 - 0.097(U - B) + 0.327X,$$

$$b = B + 1.190 + 0.049(B - V) + 0.180X,$$

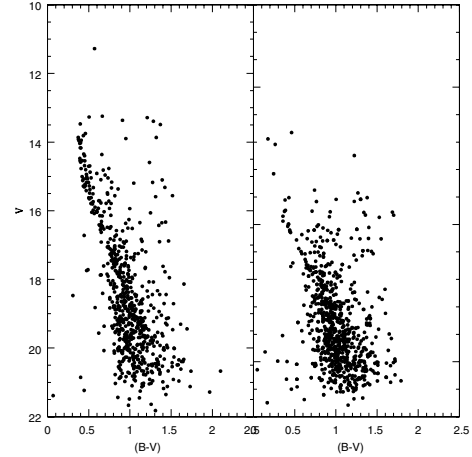
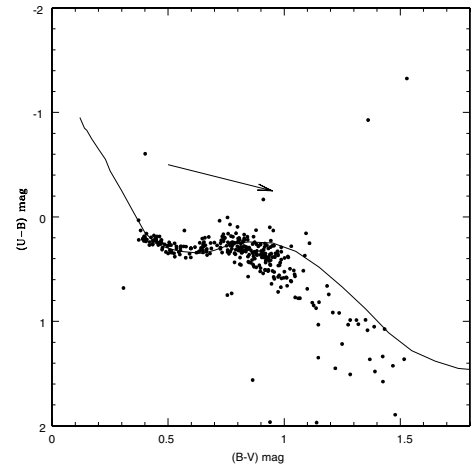
$$v = V + 0.725 - 0.060(B - V) + 0.094X.$$

The zero-point errors are 0.010, 0.013 and 0.018 mag in *V*, *B* and *U*, respectively.

We compared our photometry of NGC 7245 with that of Petry & DeGioia-Eastwood (private communication). We could identify 48 common stars. The average and the standard deviation of the difference (our data – other data) is 0.003 ± 0.025 in *V* magnitude and -0.04 ± 0.09 in $(B - V)$ magnitude. The *V*-band photometric data of King 9 were compared with those of Phelps et al. (1994). 297 stars were found to be common. The data were found to compare well for most of the stars, except for some outliers. If we ignore the outliers, the average value of the difference is 0.06 ± 0.08 in *V* magnitude.

4 NGC 7245

NGC 7245 is a sparse cluster (Fig. 1), without a well-defined centre. The adopted cluster area is indicated by the dashed lines and the

**Figure 2.** The CMDs of the cluster (left-hand panel) and the field region (right-hand panel) of NGC 7245.**Figure 3.** Estimation of reddening towards NGC 7245 using the $(U - B)$ versus $(B - V)$ diagram.

centre by the open circle. A number of bright stars were found to the left-hand side of the cluster. These stars were found to delineate the upper main-sequence (MS). Thus, the cluster region is elongated to the left-hand side to include these bright stars. King 9 is found as a faint and condensed cluster at the lower right-hand side of the field. The adopted cluster area for this cluster is also shown by the dashed lines. In order to delineate the cluster sequence from contamination by field stars, we defined a field region close to the periphery of the observed region.

The colour–magnitude diagram (CMD) of the cluster region shows a well-defined MS as compared to that of the field region (Fig. 2). $(U - B)$ versus $(B - V)$ colour–colour diagram of stars inside the cluster region (Fig. 3), is used to estimate the reddening. The fit is good for the blue side, whereas it fails in the red side. Since the MS of the cluster lies in the blue side, we fit the blue side rather than the red side. Estimated value of the reddening is 0.45 ± 0.02 mag.

To identify the cluster sequence clearly, the field stars must be removed from the cluster CMD. The brighter stars which do not share the cluster reddening are removed. For fainter stars, we statistically subtracted the field stars from the cluster CMD. The data can be assumed to be complete up to $V = 19$ mag. Since the cluster

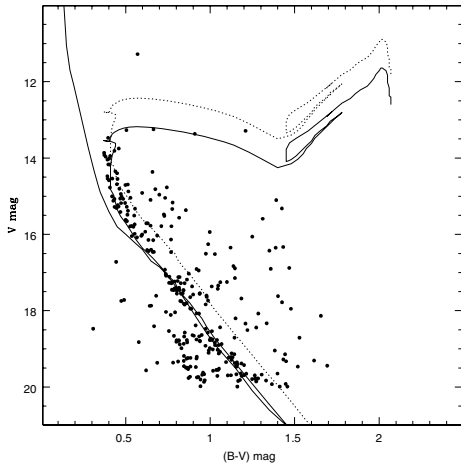


Figure 4. 400-Myr isochrone (continuous line) is fitted to the field-subtracted CMD of NGC 7245. The ZAMS is also overplotted on the CMDs. The dotted lines correspond to the isochrone for binary stars with mass ratio equal to 1.

and the field regions have the same area, the stars in the field CMD can be used to statistically remove the field stars. This is done using the zapping technique, where the candidate field stars in the cluster CMD are removed by cross-correlating the cluster CMD with the field CMD. Maximum search size used is 0.2 mag in V and 0.1 mag in $(B - V)$. In the case of NGC 7245, half of the above values were used. After this procedure, the cluster sequence gets delineated very clearly (Fig. 4). Most of the field stars found to the right-hand side of the MS are removed. On the other hand, there are some stars located to the left-hand side of the MS and fainter than $V = 18$ mag. We consider the MS which is brighter than $V = 18$ mag for the estimation of cluster parameters. Zero-age main-sequence (ZAMS) is fitted to the cluster MS to estimate a distance modulus as $(V - M_V)_0 = 12.9 \pm 0.2$ mag (distance = 3800 ± 350 pc). The above estimate is also supported by the isochrone fits to the cluster sequence. We used Bertelli et al. (1994) isochrones for solar metallicity. The age of the cluster is $\log(\text{age}) = 8.6$, which corresponds to 400 Myr. The isochrone shown as the bold line is for 400 Myr and the isochrone for the binary stars is shown as the dotted line. The evolved part of the CMD is well fitted by the isochrone. In the MS, the stars are uniformly populated between the single and the binary isochrone indicating a healthy population of binaries. There is a strong indication of an MS gap at $(B - V) \sim 0.7$ mag, which corresponds to $(B - V)_0 \sim 0.25$ mag. This could be the Bohm–Vitense gap at $(B - V)_0 = 0.25$ mag. This gap is likely to be a real feature, as it is seen even before the field star subtraction (see Fig. 2).

5 KING 9

King 9 is a compact cluster found very close to NGC 7245 in the sky. It appears to be farther and older than NGC 7245. A field area of equal size is selected from the bottom left-hand side. In the cluster CMD (left-hand panel, Fig. 5), the MS is clearly visible, in sharp contrast to the field CMD (right-hand panel, Fig. 5). Due to the faintness of the cluster, only 70 stars were detected in the U band and these stars are used to estimate the reddening (Fig. 6). The reddening is $E(B - V) = 0.37 \pm 0.04$, similar to the value found for NGC 7245. The large error in the reddening is due to the small number of cluster stars. The turn-off of the cluster MS is at ~ 18.0 mag and hence ZAMS fitting could not be used to estimate

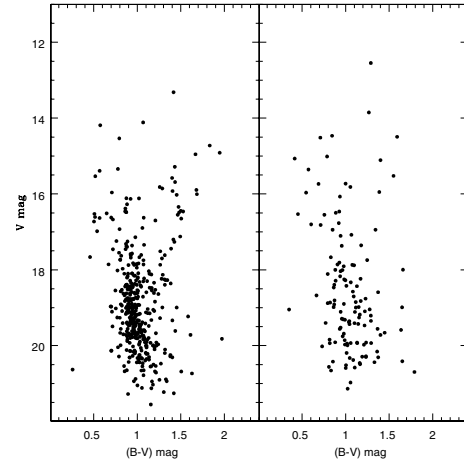


Figure 5. The CMD of the cluster region (left-hand panel) and field region (right-hand panel) of King 9.

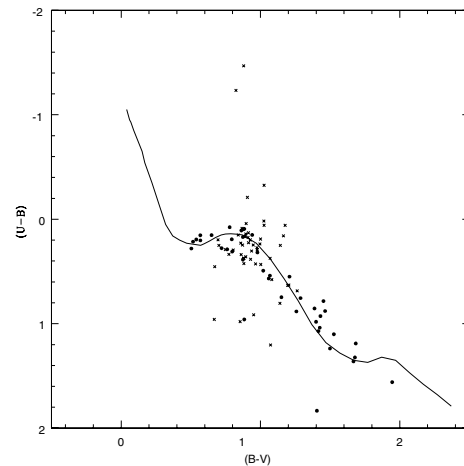


Figure 6. Estimation of reddening towards King 9 using the $(U - B)$ versus $(B - V)$ diagram. The crosses indicate stars brighter than $V = 17.5$ (likely to be field stars) and the dots indicate stars fainter than $V = 17.5$ mag (potential cluster members).

the distance. We eliminated the field stars in the King 9 cluster CMD, using a procedure similar to that adopted for NGC 7245. In the cleaned CMD (Fig. 7), MS and turn-off are very clearly visible, even though it is just 2 mag brighter than the limit of detection. The isochrone fitting to the cluster CMD is also shown. The age of the cluster is $\log(\text{age}) = 9.5$ (3.0 Gyr) and the distance modulus is 14.5 ± 0.3 mag (distance = 7.9 ± 1.1 kpc). Accordingly, we find that King 9 is the farthest open cluster in the second quadrant. The 3.0-Gyr isochrone for solar metallicity does not match the giant branch very well. It is too red to fit the observed stars. We have also shown the binary sequence (dotted isochrone), where the giant branch is fitted well. This sequence fits the stars brighter than the MS very well, indicating that the cluster may have a significant fraction of binary population including some blue stragglers. The isochrones for $Z = 0.008$ (dashed lines) fits the red clump and the giant branch well, for the same age. Therefore, this distant cluster could be metal-poor. The metal-poor isochrone estimates a reddening of 0.47 ± 0.04 mag and a distance of 7.0 ± 1.1 kpc.

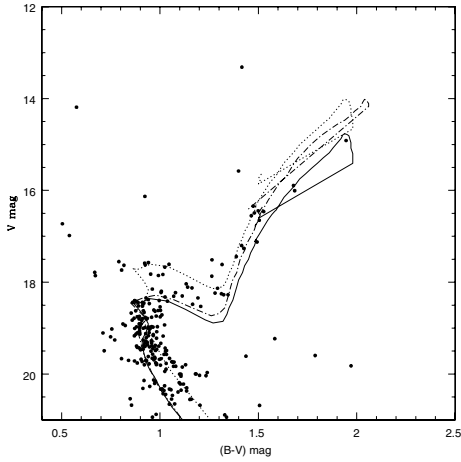


Figure 7. The field star subtracted CMD is fitted with solar metallicity isochrone of $\log(\text{age}) = 9.5$, shown as the bold line. The dotted line indicates the binary isochrone for a mass ratio of 1.0. The dashed line indicates a $Z = 0.008$ isochrone of the same age. Note that the red clump is better fitted by this isochrone.

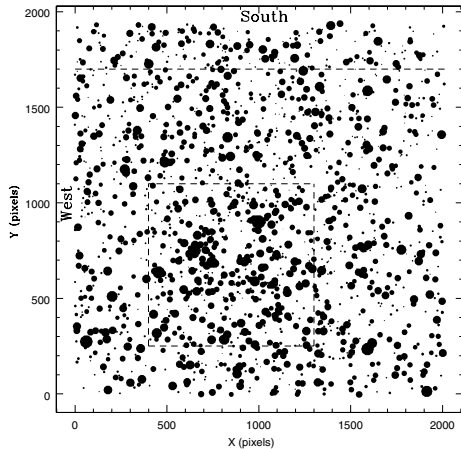


Figure 8. The observed field of King 13 along with the location of cluster and field areas.

6 KING 13

King 13 (Fig. 8) does not have a well defined centre, but a density-enhanced ring can be seen. An estimate of the cluster region is shown as the dotted line, which is about 2 arcmin from the visually estimated cluster centre. The CMDs of the cluster and the field regions (Fig. 9, left-hand and right-hand panels, respectively) show a clear MS in the cluster CMD. The fit of the reddening curve (Fig. 10) is merely satisfactory, as not many young and blue stars are found to fit the curve properly. The reddening is 0.82 ± 0.02 mag. The cleaned CMD of the cluster region is shown in Fig. 11, where the ZAMS fit and the isochrone fits are also shown. The distance modulus is 12.5 ± 0.2 mag (distance = 3100 ± 330 pc). The age of the cluster is $\log(\text{age}) = 8.5$ (age = 300 Myr).

7 IC 166

IC 166 is a rich cluster (Fig. 12) and the centre of the cluster is at $X = 917$ and $Y = 1058$. From the radial density profile, the cluster radius is estimated as 4 arcmin. We consider the central condensed

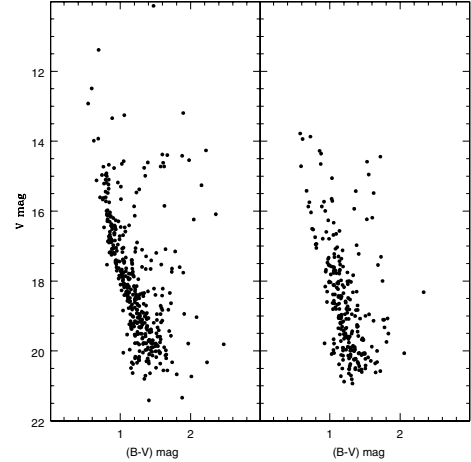


Figure 9. Observed CMD of the cluster region (left-hand panel) and field region (right-hand panel) of King 13.

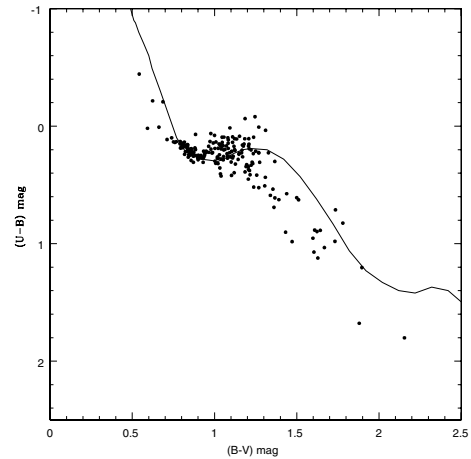


Figure 10. Estimation of reddening towards King 13 using the $(U - B)$ versus $(B - V)$ diagram.

region of the cluster within the radius of 2.5 arcmin to estimate the parameters. The region considered as field is also shown. The cluster sequence is clearly visible (left-hand panel, Fig. 13), along with a significantly elongated red clump. The CMD of the field region (right-hand panel, Fig. 13) shows a scattered sequence, with a number of bright stars, which are also seen in the cluster CMD. The reddening sequence is fitted to the red clump stars (Fig. 14), and the reddening is $E(B - V) = 0.80 \pm 0.02$ mag. The fit for the red clump stars is good, whereas it is not so good for the MS stars. The field star corrected CMD (Fig. 15) shows that the brighter stars in the CMD are removed, and the turn-off is clearly visible. Isochrone for an age of 1.0 Gyr is shown as the continuous line and its binary isochrone as the dotted line. This isochrone fits the turn-off very well. On the other hand, it fails to fit the red clump stars. Some of the brighter subgiants could be binaries as they fall on the binary isochrone. In order to fit the red clump stars, isochrone of lower metallicity ($Z = 0.008$) is also plotted (dashed line). The fit of this isochrone to the red clump stars is better, as it extends to fainter magnitudes. For a better fit, the isochrone needs to reach fainter magnitudes. This gives an indication that the cluster could be more metal-poor than $Z = 0.008$. The fit shown for solar metallicity isochrone indicates the following cluster parameters. Reddening $E(B - V) = 0.80 \pm$

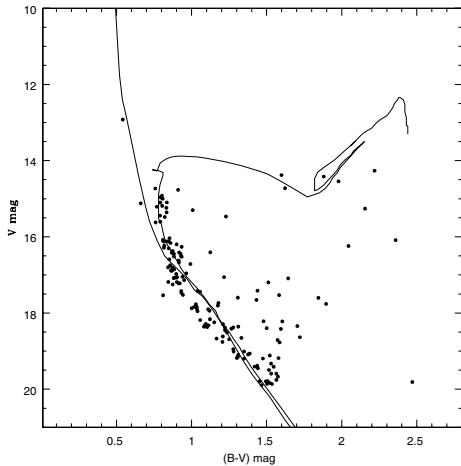


Figure 11. An age of $[\log(\text{age}) = 8.5]$ is estimated for King 13 using isochrone fit.

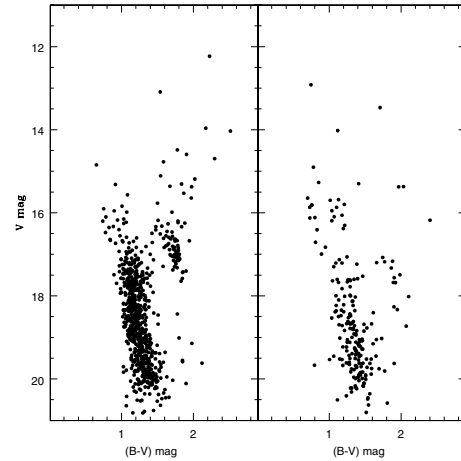


Figure 13. The cluster (left-hand panel) and field (right-hand panel) CMD of IC 166.

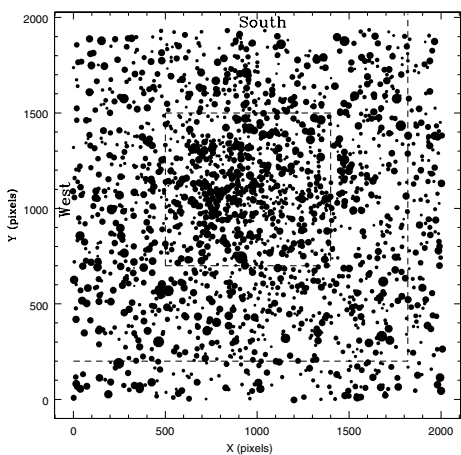


Figure 12. Observed region of IC 166 where cluster and field locations are demarcated.

0.02, distance modulus = 13.4 ± 0.2 , (distance = 4.8 ± 0.5 kpc) and an age of 1 Gyr. The fit shown for $Z = 0.008$ is obtained for the following cluster parameters. Reddening $E(B - V) = 0.92 \pm 0.02$, distance modulus = 13.2 ± 0.2 , (distance = 4.2 ± 0.5 kpc) and an age of 1 Gyr. Friel & Janes (1993) estimated the metallicity of IC 166 as $[\text{Fe}/\text{H}] = -0.32 \pm 0.20$, which was later revised to -0.41 . This supports the conclusion that the cluster is metal-poor.

8 STRUCTURE OF THE OUTER GALACTIC DISC BETWEEN $l = 90^\circ$ AND 135°

We have estimated the basic parameters of four poorly studied open clusters found in the second Galactic quadrant, between $l = 90^\circ$ and 135° . Three clusters are at a distance of about 4 kpc and one cluster is beyond 7 kpc. Here, we try to find how these clusters have contributed to the understanding of the Galactic disc in this direction, beyond 2 kpc. We have compiled the parameters of clusters in this part of the outer disc. The clusters studied here are shown as the asterisks (Fig. 16). Clusters older than 1 Gyr are not shown in the figure. Therefore, the location of King 9 is also not shown, as it is older than 1 Gyr and at a large distance. This cluster is located about 240 pc below the plane. Fig. 16(a) shows the distribution of clusters

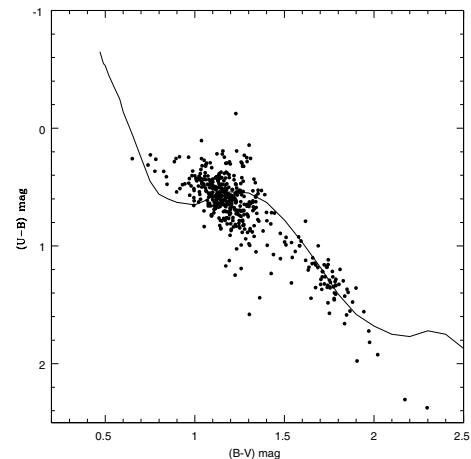


Figure 14. Estimation of reddening towards IC 166 using the $(U - B)$ versus $(B - V)$ diagram.

between $l = 90^\circ$ and 135° , as a function of their distance from the plane (Z). Fig. 16(b) shows the distribution of their distance as a function of Z . The dots indicate clusters younger than 100 Myr and the open circles indicate clusters older than 100 Myr, but younger than 1.0 Gyr. It is clear from these plots that the majority of clusters are found below the Galactic plane. One cluster, Be 93 is found at a distance of 700 pc to the north. Be 93 is just 100 Myr old. Be 93 was not considered for the calculation mentioned below. It will be interesting to study the kinematics of Be 93, in future. We estimated the average value of Z from our sample. Nineteen (32 per cent) clusters are found above and 41 (68 per cent) clusters are found below the Galactic equator. The average value of Z is -47 ± 16 pc. Thus the Galactic disc, as delineated by clusters, is bent to the south. All the four clusters studied in this paper are in the southern part of the disc. From Fig. 16(b), it is clear that these clusters have increased the number of clusters known beyond 3.0 kpc. This figure also indicates that the structure of the disc beyond 4.0 kpc is not clearly seen.

This small deviation of the Galactic disc may be considered as a mild warp in the young disc. Momany et al. (2006) derived stellar warp using red clump stars located between 2 and 4 kpc from the Sun (their fig. 8). It can be seen that the disc shows a marginal bend

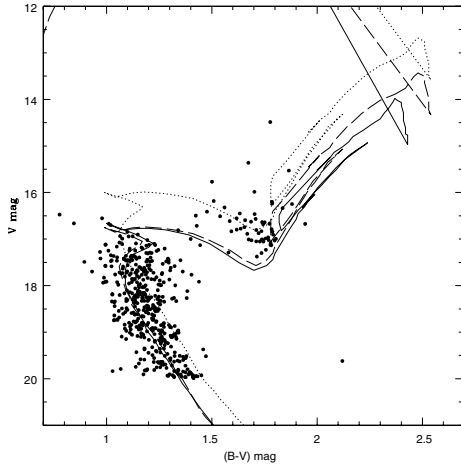


Figure 15. The field star subtracted CMD is fitted with solar metallicity isochrone of $\log(\text{age}) = 9.0$, shown as the bold line. The dotted line indicates the binary isochrone for a mass ratio of 1.0. The dashed line indicates a $Z = 0.008$ isochrone of the same age. Note that the red clump is better fitted by this isochrone.

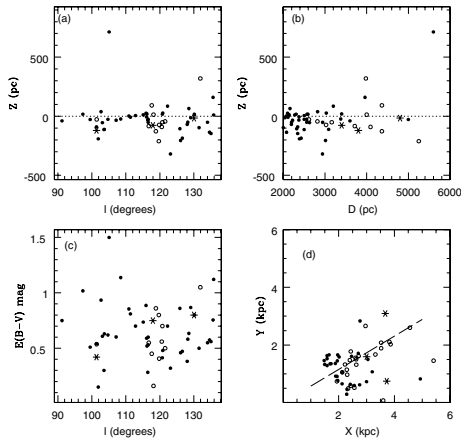


Figure 16. Distribution of clusters between $l = 90^\circ$ and 135° and beyond 2 kpc. (a) Distribution of clusters in Z (pc) as a function of the Galactic longitude, l . Clusters younger than 100 Myr are shown as the dots and clusters older than 100 Myr and younger than 1 Gyr are shown as the open circles. (b) Their distribution in Z (pc) as a function of distance D (pc). (c) Reddening distribution as a function of longitude, l . (d) Cluster distribution in the Galactic coordinates. This figure is meant to trace any spiral beyond the Perseus spiral arm. The dotted line shows the location of $l = 130^\circ$.

towards the negative latitudes. The cluster distribution might be indicating the same bend in the disc at these longitudes and at similar distances from the Sun. Thus the young disc follows the warp of the intermediate age red clump stars. It will be interesting to see the young disc beyond 4.0 kpc, as this kink seen in red clump stars disappears at larger distances. In fact, the disc bends towards the northern latitudes (Momany et al. 2006, fig. 8). Thus it is essential to increase the sample of young clusters beyond 4.0 kpc in this quadrant. Pandey, Sharma & Ogura (2006) found a similar warp between $l = 100^\circ$ and 130° when they traced the background population of open clusters in this direction (their fig. 6).

The average value of reddening increases from 90° to 135° (Fig. 16c). The reddening estimates of the clusters studied here are in agreement with those estimated for other nearby clusters. The Perseus arm stretches between 2 and 3 kpc (Fig. 16d), which is the locus of the dots representing open clusters younger than 30 Myr [equivalent to $\log(\text{age}) = 7.5$]. At $l \sim 130^\circ$, there is a stretch of clusters outwards up to a distance of ~ 5.5 kpc. The clusters found in this extension are all older than 30 Myr. Hence, this cannot be considered as an extension of the Perseus spiral arm. This figure does not support the existence of a spiral arm beyond the Perseus arm. Two of the clusters, NGC 7245 and IC 166, are found beyond the Perseus arm, while the cluster King 13 is part of the outward stretch. Pandey et al. (2006) have shown a similar extension in their fig. 6, as delineated by the background population towards open clusters.

King 9 and IC 166 are located beyond a Galactocentric radius of 10 Kpc. According to the observed radial abundance gradient of open clusters (Friel et al. 2002, fig. 2), these clusters are expected to be metal-poor ($[\text{Fe}/\text{H}] \sim -0.3$). King 9 and IC 166 also belong to an older group, as old as or older than 1 Gyr. These two clusters are important targets to derive the metallicity gradient in the disc as a function of radial distance. There are only four known open clusters, which are older than $\log(\text{age}) = 9.4$ and located beyond 7.0 kpc. Three of them are found in the third quadrant and one in the fourth quadrant. King 9, the farthest old open cluster in the second quadrant, is a potential target to study the kinematics and abundances to understand the properties of the Galactic disc at its extremes.

ACKNOWLEDGMENTS

We thank the staff of the Indian Astronomical Observatory, Hanle-Ladakh and at CREST Campus, Hosakote, for assistance during observations. This research has made use of WEBDA database, operated at the Institute of Astrophysics, University of Vienna.

REFERENCES

- Bertelli G., Bressan A., Chiosi C., Fagotto F., Nasi E., 1994, *A&AS*, 106, 275
 Burkhead M. S., 1969, *AJ*, 74, 1171
 Friel E. D., Janes K. A., 1993, *A&A*, 267, 75
 Friel E. D., Janes K. A., Tavares M., Scott J., Katsanis R., Lotz J., Hong L., Miller N., 2002, *AJ*, 124, 2693
 Karaali S., 1971, *Publ. Istanbul. Univ. No. 92*
 Marx S., Lehmann H., 1979, *Astron. Nach.*, 300, 295
 Momany Y., Zaggia S., Gilmore G., Piotto G., Carraro G., Bedin L. R., de Angeli F., 2006, *A&A*, 451, 515
 Pandey A. K., Sharma S., Ogura K., 2006, *MNRAS*, 373, 255
 Phelps R. L., Janes K. A., Montgomery K. A., 1994, *AJ*, 107, 1079
 Stetson P. B., 1987, *PASP*, 99, 191
 Vallenari A., Carraro G., Richichi A., 2000, *A&A*, 353, 147
 Viskum M., Hernandez M. M., Belmonte J. A., Frandsen S., 1997, *A&A*, 328, 158
 Yilmaz F., 1970, *A&A*, 8, 213

This paper has been typeset from a $\text{T}_{\text{E}}\text{X}/\text{L}^{\text{A}}\text{T}_{\text{E}}\text{X}$ file prepared by the author.